

AN ADAPTIVE CONTROL METHOD FOR ULTRASOUND PROSTATE HYPERTHERMIA

Lei Sun¹, Jeffery Schiano², and Nadine Barrie Smith^{1,3}

¹Department of Bioengineering, ²Department of Electrical Engineering, ³Acoustics Program, Pennsylvania State University, University Park, USA, 16802

Abstract

For thermal treatment of prostate diseases, an ultrasound phased array was designed and operated with a computer controlled amplifier system which adjusted the power and phase of each transducer element. The clinical application of such a system is to increase the temperature in the prostate to 43-45°C and maintain the temperature for 30-60 minutes for a hyperthermia therapy treatment. In this paper, an adaptive self-tuning regulator (STR) controller has been designed and implemented with this hyperthermia system using a negative feedback transfer operator and a feedforward transfer operator. The transfer operators' parameters were obtained directly from plant input and output with recursive least square estimation (RLSE). The advantage of this controller was that it did not need *a priori* knowledge of the tissue properties and could adaptively change its control variables according to the perfusion rate or other dynamic properties. Simulations indicated that the prostate reached the target temperature without overshoots and oscillations within 100 seconds. The system also successfully adapted to the dynamic tissue properties. Phantom experiments showed that the measured temperature tracked the reference temperature closely and reached the target temperature with a little oscillations and without overshoots within 150 seconds, which was consistent with the computer simulations.

Key Words: self-tuning regulator, ultrasound hyperthermia, prostate disease

1. Introduction

Diseases associated with the prostate gland include benign prostate hyperplasia (BPH) and prostate cancer. Although surgery is the current treatment, older men often have additional health problems, which rule out surgery as a viable option. Ultrasound hyperthermia treatment, which is to increase the tissue temperature to 43-45°C for 30-60 minutes, has been used clinically and have shown effectiveness for the prostate treatment when it is associated with radiotherapy or chemotherapy [1-4]. Hyperthermia can enhance radiotherapy by preventing cellular repair mechanisms from radiation induced injury and is effective in killing hypoxic cells, which are resistant to radiation therapy [5].

However, in the clinical treatments, the temperature distribution is controlled by a clinician's intervention and judgment through adjusting the power to the array elements based on temperature information from thermocouples placed in the prostate. Previously, various control strategies have been designed for controlling temperature in either actual or simulated hyperthermia treatment, such as proportional-integral (PI) bang-bang control [6], reduced-order multi-input multi-output (MIMO) control [7], adaptive MIMO control [8], multipoint adaptive control [9], linear quadratic regulator (LQR) [10], magnetic resonance imaging (MRI) compatible single input single output (SISO) PI control [11]. The purpose of this research is to introduce an adaptive feedback control method for ultrasound hyperthermia treatment to achieve the desired prostate temperature with minimal overshoots, rapid rise time, fast settle time, and small oscillations.

2. Materials and Methods

2.1 The Ultrasound Hyperthermia System

The ultrasound hyperthermia system consisted of an ultrasound phased array driven by a computer controlled amplifier system (Fig. 1) [4;10-15]. *In vitro* prostate phantom experiments used a 16-element ultrasound unfocused array immersed in a Plexiglas[®] tank (25 x 38 x 53 cm³) filled with distilled degassed water. The array was driven by a programmable 64-channel radio frequency (RF) amplifier (Advanced Surgical System Incorporated, Tucson, AZ) connected to the computer through a RS-232 port [16;17]. Temperatures change within the *in vitro* phantom was determined by a multi-element fiber optic thermometer (Luxtron Corporation, Mountain View, CA) inserted in the prostate phantom. Each probe was shielded with copper tube to prevent heat absorption of the ultrasound by the probe [18]. The prostate phantom was made of agar powder simulating the response of human tissue to capture the temperature of the heated tissue [19]. The adaptive feedback control algorithm was used to maintain a desired temperature evolution by controlling the electrical power of the individual phased array element.

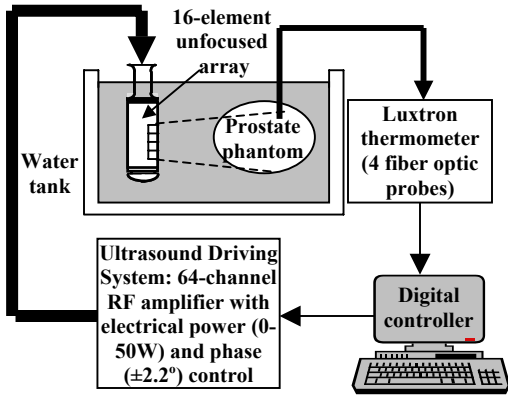


Figure 1. Block diagram of the ultrasound hyperthermia system. A 16-element ultrasound array driven by a computer controlled amplifier generates acoustic energy to heat the tissue phantom. The heating in the prostate phantom is monitored by a fiber optic thermometer which sends temperature information to digital controller.

2.2 Control Simulations

2.2.1 Pressure Field Calculation

Simulations were initially performed before *in vitro* experiments to determine the control variables such as the reference model parameters and tissue thermal response to heat from the ultrasound wave by a 64-element phased array [20]. The acoustical pressure of the array was calculated by modeling every element of the array as an independent simple source and summing the contribution of each simple source at each point in the field. The acoustic pressure $p(x,y,z)$ at a specific point (x,y,z) in the field due to a simple source was calculated using the Rayleigh-Sommerfeld equation [21]:

$$p_i(x,y,z) = \sqrt{\frac{2W\rho}{cA}} \left(\frac{fS}{d}\right) e^{\{(\phi - \frac{2\pi d}{\lambda})i - d\alpha\}} \quad (1)$$

where W is total acoustical power output from the array, ρ is density of the medium (998 kg/m^3), c is speed of sound in the medium (1500 m/s), A is total transducer surface area, f is frequency (1.2 MHz), S is area represented by the simple source, d is distance from the source to the point (x,y,z) , ϕ is phase of the simple source, λ is wavelength and α is attenuation in the medium ($10 \text{ Np/(m}\cdot\text{MHz)}$).

The net pressure due to all the elements was determined by summing the effects of each simple source:

$$P_{net}(x,y,z) = \sum_{i=1}^n p_i(x,y,z) \quad (2)$$

and net power deposition at point (x,y,z) was the result of the attenuation [22]:

$$q(x,y,z) = \frac{\alpha P_{net}^2(x,y,z)}{\rho c} \quad (3)$$

Two pressure fields were calculated by Matlab[®] program (Mathworks Incorporated, Natick, MA) in an $8 \times 8 \times 4 \text{ cm}^3$ three-dimensional (3-D) volume 1.5 cm away from the array surface. The first was a single focus pattern where the focal point was at $(0, 0, 2.5 \text{ cm})$ given that the center of the array was the origin and z -axis was

perpendicular to the array surface. The other was a four foci pattern with all the foci at $(0.3, 0.3, 3 \text{ cm})$. Each focus was generated by a quarter of the array on a symmetric way. The phase of each element of the array was determined by:

$$\phi_i = \frac{360^\circ}{\lambda} (d_i - d_0) - 360^\circ n \quad (4)$$

where ϕ_i is phase of element i in degrees, d_i is distance from the center of element i to the focus, d_0 is the focus depth, n is an integer used to maintain $0 < \phi_i < 360^\circ$.

2.2.2 Thermal Model of Tissue

The nature of heat transfer in tissue field was determined by applying Pennes' bioheat transfer equation (BHTE) [23;24]. The three dimensional representation of this equation in Cartesian coordinates is:

$$\rho c_t \frac{dT}{dt} = \kappa \left(\frac{d^2 T}{dx^2} + \frac{d^2 T}{dy^2} + \frac{d^2 T}{dz^2} \right) - w c_b (T - T_a) + q(x,y,z) \quad (5)$$

where ρ is density (998 kg/m^3), c_t is specific heat of the tissue ($3770 \text{ J/(kg }^\circ\text{C)}$), κ is thermal conductivity ($0.5 \text{ W/(m}^\circ\text{C)}$), T is temperature at time t and point (x,y,z) , T_a is arterial blood temperature (37°C), w is perfusion rate (in $\text{kg/m}^3\text{s}$), c_b is specific heat of the blood ($3770 \text{ J/(kg}^\circ\text{C)}$) and $q(x,y,z)$ is the power deposited (Equ. 3) at the point (x,y,z) in the tissue. Although it is widely used, this implementation neither accounts for variations in tissue, such as the presence of blood vessels, nor for any spatial or temporal variation in perfusion levels. Therefore, it does not provide a "perfect" model for the behavior of tissue targeted with the acoustical power of an ultrasound array. However, it is adequate to estimate the effectiveness of the different controllers.

The BHTE was solved using a 3-D numerical finite difference equation with Compaq Fortran 6.0 (Compaq Computer Corporation, Houston, TX) programming language and all boundary and initial conditions were set to 36.8°C . A time step of 1 second and a grid spacing of $1 \times 1 \times 1 \text{ mm}^3$ were used for the temporal and spatial resolution of the BHTE implementation. The 1 second sampling period was the fast period the system can achieve.

2.2.3 The Self-Tuning Regulator Method

The BHTE (Equ. 5) indicates a nonlinear relationship between the power and the temperature, and therefore, it is difficult to apply the existing control theories. For simplicity, an assumption was made such that the power and the temperature satisfied an autoregressive moving average (ARMA) model with unknown orders and coefficients. The assumed ARMA model is:

$$A(q)y(k) = B(q)u(k) \quad (6)$$

where $y(k)$ is the temperature output and $u(k)$ is the command power input. A and B are polynomials in the forward shift operator q . The system transfer function is $B(z)/A(z)$. The polynomials A and B have the degrees:

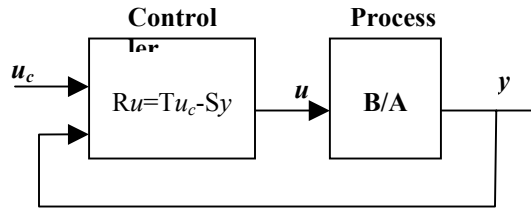


Figure 2. A general linear controller with two degrees of freedom. B/A is the transfer function of the process. A and B are relative prime and A is also assumed monic. R, S and T are control polynomials to achieve desired performance of the closed-loop system.

$$\deg A = n \quad (7)$$

$$\deg B = \deg A - d_0 = n - d_0 \quad (8)$$

where parameter n denotes the order of polynomial A and parameter d_0 represents the integer part of ratio of time delay and sampling period. Further assumptions were that A and B were relatively prime and A was monic, that was, the coefficient of the highest power in A was unity.

An adaptive self-tuning regulator control method was proposed based on the ARMA model assumption. This control method could converge the measured temperature to the reference temperature. An interesting result is that this could happen even if the model structure is incorrect.

A general linear controller can be described by:

$$Ru(k) = Tu_c(k) - Sy(k) \quad (9)$$

where R, S and T are polynomials. This control law represents a negative feedback with the transfer operator equal to $-S/R$ and a feedforward with the transfer operator equal to T/R . With the feedback and feedforward, this model has two degrees of freedom (Fig. 2).

Elimination of $u_c(k)$ between Equ. 6 and 9 gives the following equations for the closed-loop system:

$$y(k) = \frac{BT}{AR + BS} u_c(k) \quad (10)$$

$$u(k) = \frac{AT}{AR + BS} u_c(k) \quad (11)$$

The close-loop characteristic polynomial A_c is thus,

$$AR + BS = A_c \quad (12)$$

The key idea of the design method was to specify the desired closed-loop characteristic polynomial A_c . The polynomials R and S could then be solved from Equ. 12. The significance of the design procedure for polynomial A_c was that it was considered to be a design parameter that was chosen to give the desired properties to the closed-loop system. Equ. 12 played a fundamental role in algebra, which is called *Diophantine* equation, and always has solutions if the polynomials A and B do not have

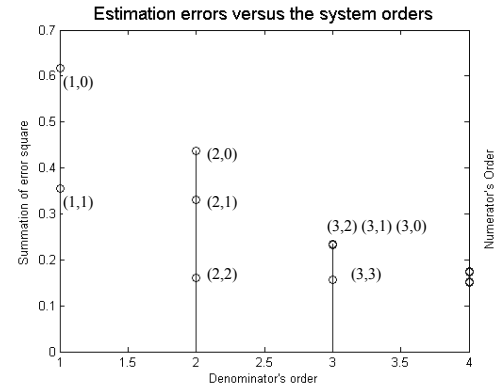


Figure 3. The system estimation errors versus the system order. The first number in parenthesis is the denominator's order, the second number is the numerator's.

common factors. With direct self-tuning regulators, the model parameters A and B did not need to be solved. The controller polynomials R, T and S could be obtained directly from plant input $u(k)$ and output $y(k)$ using recursive least square estimation (RLSE).

2.2.4 Control Simulations and Experiments

For the simulations, the first 20 seconds of the hyperthermia treatment was used to estimate the initial STR control parameters. The excitation signal for estimation was a square wave with period of 4 seconds switching between 0 and 1 Watt to guarantee the persistency of the excitation. After 20 seconds, the control parameters were updated every 1 second with new $u(k)$ and $y(k)$ data using RLSE, then the controller calculated the power level of the array and outputted it to each array element at the same rate. The reference temperature was an exponential signal with a time constant of 15 seconds.

The control experiments followed the same procedure as the simulations. Since the 64-element array was not available yet, another 16-element unfocused array was applied. The SISO STR experiments were conducted with one element of the array and one fiber optic probe. The STR control algorithm coded in Microsoft Visual Basic 6.0 (Microsoft Corporation, Redmond, WA) manipulated the real time heating process. The sampling period was also chosen to be 1 second to make the control as fast as possible.

3. Results

3.1 The Second Order ARMA Model Assumption

Figure 3 plots the system estimation errors versus the system orders using experimental data. The numbers in parenthesis represent the transfer function denominator and numerator's order, respectively. Figure 3 shows that at orders larger than (2,2) increasing the order number can not decrease the estimation errors, which means the system was a second order system.

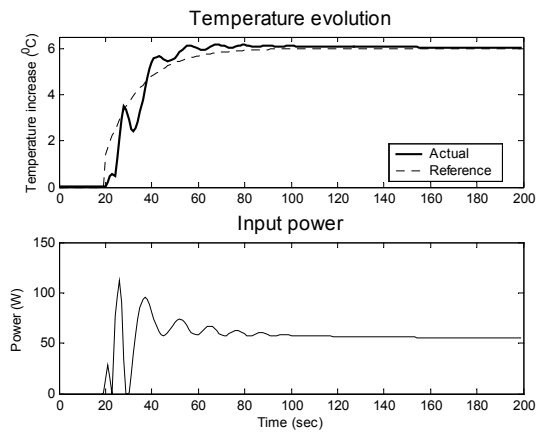


Figure 4. Temperature evolution (top) and input power (bottom) for SISO STR control with constant perfusion rate $2.0 \text{ kg/m}^3\text{s}$.

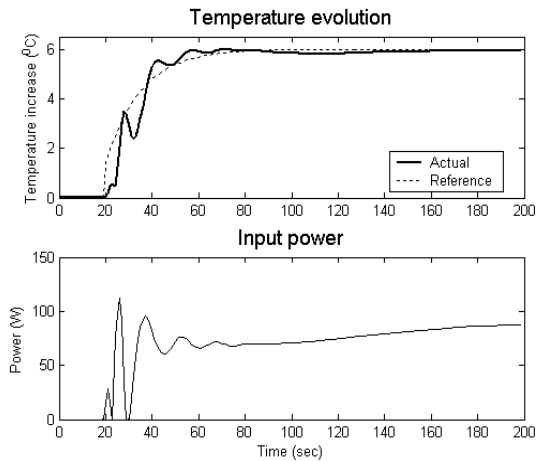


Figure 5. Temperature evolution (top) and input power (bottom) for SISO STR control with linearly changing perfusion rate.

3.2 Single Input Single Output Control Simulations

The SISO STR control simulations were conducted under two control conditions. One was at constant perfusion rate of $2.0 \text{ kg/m}^3\text{s}$, and the other was at linearly increasing perfusion rate changing from $2.0 \text{ kg/m}^3\text{s}$ at 20 seconds to $20.0 \text{ kg/m}^3\text{s}$ at 180 seconds. Figure 4 shows the measured temperature change from 0 to 200 seconds (top graph) and the array's input power level from 0 to 200 seconds (bottom graph) at constant perfusion rate. From 20 to 80 seconds, the measured temperature approached the reference temperature quickly. At 100 seconds the temperature reached its steady state point, and maintained it for the last 100 seconds without oscillations. The input power ranged from 0 to about 100 Watts (W) and after 100 seconds it reached a constant value of 55 W. This was reasonable because when the temperature reached its equilibrium point, the input power compensated the heat loss of the tissue to its surrounding environments.

Figure 5 shows the measured temperature evolution (top) and input power (bottom) at linearly increasing perfusion rate. The temperature evolution in Fig. 5 is similar with that in Fig. 4 during the first 80

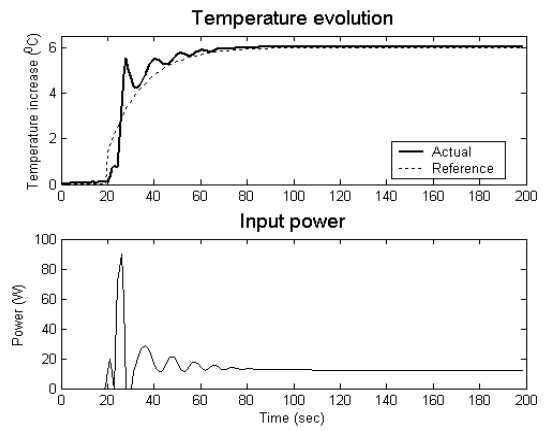


Figure 6. Average temperature evolution (top) and input power (bottom) for MIMO STR control with constant perfusion rate $2.0 \text{ kg/m}^3\text{s}$.

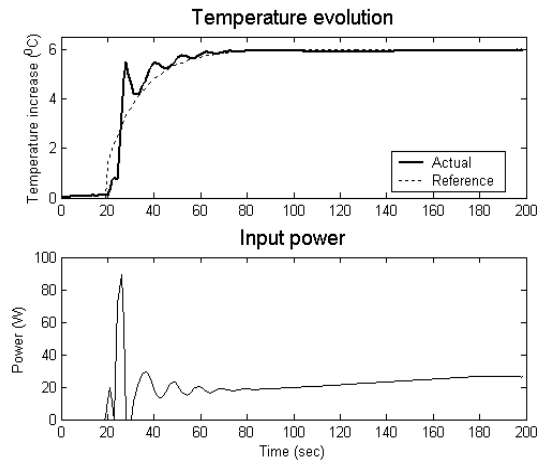


Figure 7. Average temperature evolution (top) and input power (bottom) for MIMO STR control with linearly changing perfusion rate.

seconds when the perfusion rate was small. From 100 to 160 seconds, a concave curve was present due to the fact that the large perfusion rate was not compensated enough by the input power. After 160 seconds, the temperature reached the steady state when the input power balanced the heat loss completely. The steady state values difference between Fig. 4 and 5 could be explained by the fact that more energy was needed when blood removed more energy from the hot spot at larger perfusion rate.

3.3 Multiple Input Multiple Output Control Simulations

In the four foci pattern hyperthermia, the controller was multi-input multi-output (MIMO). To avoid complex matrix operation, one temperature was obtained by averaging the 4 foci's temperatures. As a result, the MIMO control was transformed to a single input multiple output (SIMO) control. Furthermore, the SIMO was simplified to a SISO control because the 4 output power levels were identical due to the symmetry. Without any modification, the SISO STR control method could be applied to this MIMO control.

Figure 6 shows the average temperature evolution (top) and input power (bottom) at constant

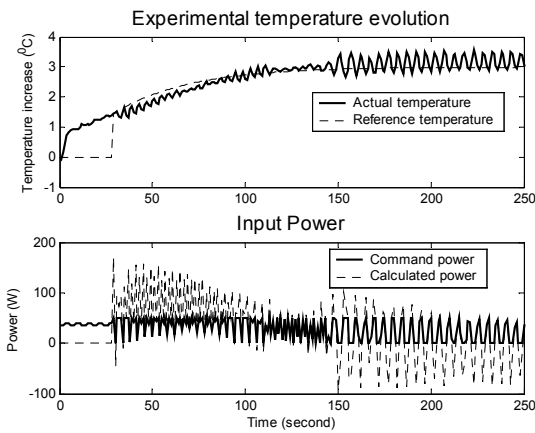


Figure 8. The SISO STR experimental results with phantom.

perfusion rate $2.0 \text{ kg/m}^3\text{s}$. The MIMO STR simulations showed similar results with the SISO STR control simulations. The measured temperature rapidly rose to the target temperature within 100 seconds, and maintained the target temperature without oscillations and overshoots. The input power had a larger dynamic range than the SISO STR control simulations because the four foci pattern had larger grating lobes, which affected the focal points more.

Figure 7 shows the average temperature evolution (top) and input power (bottom) at linearly increasing perfusion rate changing from 2.0 to $20.0 \text{ kg/m}^3\text{s}$. The perfusion rate affected the MIMO control the same manner as it did on the SISO control. However, the concave part of the temperature evolution from 100 to 160 seconds was less significant, mainly because of the interchange of the energy with the other three foci offset the heat loss due to the blood flow. Both the focal area and focal length of the MIMO control were increased substantially resulting in a much larger heating volume also because of the multiple foci. Decreasing the number of the hyperthermia treatments would result in decreasing the total treatment time, therefore the multiple foci treatment would be very useful in clinical treatment.

3.4 SISO STR Control Experimental Results

The control parameters were estimated at the first 30 seconds with a square wave switching from 35 to 40 W with period of 6 seconds. During the estimation period, the phantom was also heated to 38.5°C . The reference temperature was an exponential signal with a time constant of 40 seconds.

Figure 8 plots the temperature evolution (top) and the input power (bottom) as a function of time. After 150 seconds the actual temperature reached the set point and maintained the set point temperature for 100 seconds without overshoots and a little oscillations. The rising time of this experiment was larger than the simulations, simply because the dynamic range of the amplifier driving the array was from 0 to 50 W. The time constant of the reference exponential signal had to be kept large,

otherwise the amplifier would saturate easily. Increasing the acoustic intensity at focal point could be a good solution to the amplifier saturation. Even though the rising time could not be smaller, compared to the 30-60 minutes clinical hyperthermia treatment, 150 seconds settling time achieved in this experiment was still desirable.

4. Discussion

Simulations and experiments have shown that the temperature evolution at specific points several centimeters deep inside the tissue could be elevated precisely using the self-tuning regulator control algorithm. The results also showed that the STR method adaptively dealt with the time-varying disturbances such as perfusion rate quite well.

The simulations indicated that under the STR control method, the actual temperature converged to the reference temperature within 100 seconds with small errors. There were no overshoots and little oscillations in the simulation results. An advantage of this control method was that it did not require *a priori* knowledge. Therefore, there was no need to choose control variables before the hyperthermia treatment.

Compared the simulation results of the single focus pattern with the four foci pattern, the latter heated a much larger volume of the prostate. It is encouraging that the multiple foci pattern will save the total treatment time and make patients more comfortable in clinical hyperthermia treatment.

Phantom experiments showed that the measured temperature tracked the reference temperature closely, which was consistent with the computer simulations. However, temperature oscillations happened at the last part of the hyperthermia treatment. One reason is that the second order model assumption was not valid once the temperature reached its steady state. Another reason is that the amplifier was easily saturated due to the low intensity of the 16-element unfocused array.

These results indicate that the adaptive controller responded well to dynamic biological changes simulated to a true clinical procedure, however more research will be performed to verify the *in vivo* case.

5. Acknowledgement

This work was funded by Whitaker Foundation.

References

- [1] Stawarz, B., Szmigielski, S., Ogrodnik, J., Astrahan, M., and Petrovich, Z., A comparison of transurethral and transrectal microwave hyperthermia in poor surgical risk benign prostatic hyperplasia patients, *J. Urology*, vol. 146, 1991, 353-357.

- [2]Strohmaier, W. L., Bichler, K. H., Bokcing, A., and Fluchter, S. H., Histological effects of local microwave hyperthermia in prostatic cancer, *Int. J. Hyperthermia*, vol. 7(1), 1991, 27-33.
- [3]Fosmire, H., Hynynen, K., Drach, G. W., Stea, B., Swift, P., and Cassidy, R., Feasibility and toxicity of transrectal ultrasound hyperthermia treatment of locally advanced adenocarcinoma of the prostate, *Int. J. Rad. Onc., Biol., Phys.*, vol. 26, 1993, 253-259.
- [4]Hurwitz, M. D., Kaplan, I. D., Svensson, G. K., Hanson, J. L., and Hynynen, K., Feasibility and patient tolerance of a novel transrectal ultrasound hyperthermia system for treatment of prostate cancer," *Int. J. Hyperthermia*, vol. 17(1), 2001, 31-37.
- [5]Overgaard, J. and Overgaard, M., Hyperthermia as an adjuvant to radiotherapy in the treatment of malignant melanoma, *Int. J. Hyperthermia*, vol. 3(6), 1987, 483-501.
- [6]Lin, W., Roemer, R. B., and Hynynen, K., Theoretical and experimental evaluation of a temperature controller for scanned focused ultrasound hyperthermia, *Med. Phys.*, vol. 17(4), 1990, 615-625.
- [7]Potocki, J. K. and Tharp, H. S., Reduced-order modeling for hyperthermia control, *IEEE Transactions on Biomedical Engineering*, vol. 39(12), 1992, 1265-1273.
- [8]Hartov, A., T.A.Colacchio, J.W.Strohbehn, T.P.Ryan, and P.J.Hoopes, Performance of an adaptive MIMO controller for a multiple-element ultrasound hyperthermia, *Int. J. Hyperthermia*, vol. 9(4), 1993, 563-579.
- [9]VanBaren, P. and Ebbini, E., Multipoint Temperature Control During Hyperthermia Treatments: Theory and Simulation, *IEEE Transactions on Biomedical Engineering*, vol. 42(8), 1995, 818-827.
- [10]Hutchinson, E., Dahleh, M., and Hynynen, K., The feasibility of MRI feedback control for intracavitary phased array hyperthermia treatments, *Int. J. Hyperthermia*, vol. 14(1), 1998, 39-56.
- [11]Smith, N. B., Merrilees, N. K., Dahleh, M., and Hynynen, K., An MRI compatible intracavitary ultrasound array for thermal treatment of prostate disease, *Int. J. Hyperthermia*, vol. 17(3), 2001, 271-282.
- [12]C. J. Diederich and E. C. Burdette, Transurethral ultrasound array for prostate thermal therapy: initial studies, *IEEE Transactions on Ultrasonics, Ferroelectrics, and Frequency Control*, vol. 43(6), 1996, 1011-1022.
- [13]Douglas R.Daum and Kullervo Hynynen, A 256-Element Ultrasonic Phased Array for the Treatment of Large Volume of Deep Seated Tissue, *IEEE Transactions on Ultrasound, Ferroelectrics and Frequency Control*, vol. 46(5), 1999, 1254-1268.
- [14]Smith, N. B., Buchanan, M., and Hynynen, K., Transrectal ultrasound applicator for prostate heating monitored using MRI thermometry, *Int. J. Radiat. Oncol., Biol., Phys.*, vol. 43(1), 1999, 217-225.
- [15]Sokka, S. D. and Hynynen, K., The feasibility of MRI-guided whole prostate ablation with a linear aperiodic intracavitary ultrasound phased array, *Phys. Med. Biol.*, vol. 45(11), 2000, 3373-3383.
- [16]Buchanan, M. and Hynynen, K., Design and experimental evaluation of an intracavitary ultrasound phased array for hyperthermia, *IEEE Transactions on Biomedical Engineering*, vol. 41(12), 1994, 1178-1187.
- [17]Daum, D. R., Buchanan, M. T., Fjield, T., and Hynynen, K., Design and Evaluation of a Feedback Based Phased Array for Ultrasound Surgery, *IEEE Transactions on Ultrasound, Ferroelectrics and Frequency Control*, vol. 45(2), 1998, 431-438.
- [18]Hynynen, K. and Edwards, D. K., Temperature measurements during ultrasound hyperthermia, *Med. Phys.*, vol. 16(4), 1989, 618-626.
- [19]Payne, A., Mattingly, M., Shelkey, J., Scott, E., and Roemer, R. B., A Dynamic two-dimensional Phantom for Ultrasound Hyperthermia Controller Testing," *Int. J. Hyperthermia*, vol. 17(2), 2001, 143-159.
- [20]Saleh, K. and Smith, N. B. Two dimensional ultrasound phased array for thermal treatment of prostate cancer, *Proc. Ultrasonic Transducer Engineering Conference 2001 of NIH Resource on Medical Ultrasonic Transducer Technology*, University Park, USA, 2001.
- [21]Goodman, J. W., *Introduction to Fourier Optics*, (New York: McGraw-Hill, 1968).
- [22]Seip, R., VanBaren, P., Cain, C. A., and Ebbini, E. S., Noninvasive Real-Time Multipoint Temperature Control for Ultrasound Phased Array Treatments, *IEEE Transactions on Ultrasonics, Ferroelectrics, and Frequency Control*, vol. 43(6), 1996, 1063-1073.
- [23]Pennes, H. H., Analysis of tissue and arterial blood temperatures in the resting human forearm, *Journal of Applied Physiology*, vol. 1(2), 1948, 93-122.
- [24]Sapareto, S. A. and Dewey, W. C., Thermal dose determination in cancer therapy, *International Journal of Radiation Oncology-Biology and Physics*, vol. 10, 1984, 787-800.